Express Polymer Letters Vol.17, No.4 (2023) 449–456
Available online at www.expresspolymlett.com
https://doi.org/10.3144/expresspolymlett.2023.32

Research article

Modification of PEDOT:PSS films using ZnI_2 additive for power conversion efficiency enhancement of organic solar cells

Sucheewan Krobthong[1], *Sutthipoj Wongrerkdee*[1*], *Sawitree Wongrerkdee*[2], *Khathawut Lohawet*[3], *Anusit Kaewprajak*[3], *Pisist Kumnorkaew*[3]

[1]Department of Physics, Faculty of Liberal Arts and Science, Kasetsart University Kamphaeng Saen Campus, Kamphaengsaen, 73140 Nakhon Pathom, Thailand
[2]Faculty of Engineering, Rajamangala University of Technology Lanna Tak, Muang, 63000 Tak, Thailand
[3]National Nanotechnology Center, National Science and Technology Development Agency, Thailand Science Park, Khlong Luang, 12120 Pathum Thani, Thailand

Received 13 September 2022; accepted in revised form 24 November 2022

Abstract. Organic solar cells (OSCs) fabricated with poly(3,4-ethylenedioxythiophene) polystyrene sulfonate (PEDOT:PSS) films often have limited performance due to high sheet resistances since commercial PEDOT:PSS contains a high insulating PSS to conducting PEDOT ratio. To resolve this issue, zinc iodide (ZnI_2) additive was utilized to modify PEDOT:PSS films, which was carried out by mixing ZnI_2 with PEDOT:PSS solution. The mixture was deposited on a fluorine-doped tin oxide substrate to derive the modified PEDOT:PSS films for application as a hole-transporting layer in OSCs. This resulted in an enhanced power conversion efficiency for OSCs fabricated with modified PEDOT:PSS films. The enhancement was primarily due to the improved PEDOT:PSS/PCDTBT:$PC_{70}BM$ (poly[*N*-9′-heptadecanyl-2,7-carbazole-alt-5,5-(4′,7′-di-2-thienyl-2′,1′,3′-benzothiadiazole)] – PCDTBT, [6,6]-phenyl-C_{71}-butyric acid methyl ester – $PC_{70}BM$) interfaces, which facilitates enhanced hole collection performance and results in a high current density for OSC devices. Moreover, the ZnI_2 plays a role in the depletion of insulating PSS from the film's surface. This behavior causes lower sheet resistance and results in an increased J_{sc} and V_{oc} for OSC devices. Therefore, the improved interfacial contact and depletion of PSS are considered synergistic functions for OSC enhancement.

Keywords: *nanomaterials, zinc iodide, hole transporting layers, organic solar cells*

1. Introduction

Energy is a vital factor for consumption and development. The usability of conventional energy resources, including coal, oils, and natural gases, is associated with limited reserves and pollution. Therefore, alternative energy has been extensively investigated and developed for next-generation energy consumption. Solar cells are an interesting alternative technology and have been considered a candidate for sustainable technology since they are inexpensive and can be installed anywhere. The electricity generated from solar cells not only has on-grid usability but can also be stored by batteries for off-grid or hybrid systems. Furthermore, no pollution emission is associated with generating electricity using solar cells. In comparison to silicon solar cells, organic solar cells (OSCs) are developed based on a low-temperature process, no vacuum system requirements, and flexible thin film deposition, which can be easily fabricated [1–4]. A conductive polymer, poly(3,4-ethylenedioxythiophene)-poly(styrene sulfonate) (PEDOT:PSS), has been widely investigated

*Corresponding author, e-mail: sutthipoj.s@gmail.com

in OSCs, attributable to its high electrical conductivity and transparency [5, 6]. However, PEDOT:PSS chains contain high ratios of insulating PSS to conducting PEDOT, which may potentially limit the conductivity for optoelectronic device applications, including OSCs [7, 8]. Moreover, the formation of PEDOT:PSS chains might be shortly formed by thin film fabrication. To solve this issue, many researchers have focused on the development and optimization of PEDOT:PSS films. Hussain *et al.* [9] developed MXene/WO_3 embedded PEDOT:PSS hole transporting layers (HTLs) and applied them to perovskite solar cells. They prepared the MXene/WO_3 hybrid structure using a solution process. The hybrid structure was used to modify PEDOT:PSS for applying HTLs of PSCs. The PSC devices demonstrated a power conversion efficiency (*PCE*) enhancement of 12.26%. This is caused by the appropriate energy band alignment in the modified HTLs, which results in a more efficient charge transfer and a shorter carrier lifetime. Gemeiner *et al.* [10] modified PEDOT:PSS using secondary dopants of ethylene glycol (EG), polyethylene glycol (PEG), and dimethyl sulfoxide (DMSO) for dye-sensitized solar cells (DSSCs). The dopants were added to PEDOT:PSS inks and printed on fluorine-doped tin oxide (FTO) substrates. The secondary dopants caused low sheet resistance and better wettability and electrochemical activity for PEDOT:PSS films. This demonstrated efficiency enhancement for DSSCs fabricated with PEDOT:PSS counter electrodes. Wan *et al.* [11] reported an enhancement of OSCs using thionyl chloride ($SOCl_2$) treatment. PEDOT:PSS films were soaked onto $SOCl_2$. After 10 min of soaking, the PEDOT:PSS was washed with de-ionized water and isopropanol, followed by baking at 80 °C for 15 min. The $SOCl_2$-treated PEDOT:PSS was then applied as the HTL layer for the OSCs within a high *PCE* of 15%. The *PCE* enhancement was due to the $SOCl_2$ treatment, which caused an improvement in optical transparency, electrical conductivity, Seebeck coefficient, and work function. Moreover, Xu *et al.* [12] demonstrated that a co-development of an engineering fabrication using layer-by-layer and solvent treatment greatly enhanced OSC performance. The *PCE*s of fabricated OSC devices using layer-by-layer fabrication and treatment with 1-chloronaphthalene (CN) can be enhanced from 13.67 to 15.81%. These results suggest that the development strategy, including the method and treatment of PEDOT:PSS HTL, can potentially enhance OSC performance.

In this work, PEDOT:PSS films were modified using a ZnI_2 additive. The ZnI_2 is easily soluble in water to form Zn^{2+} and I^- ions, that could react with PEDOT:PSS molecules. Due to the insulating PSS parts of PEDOT:PSS causing low electrical properties, the reaction between the ZnI_2 additive and PEDOT:PSS reduces the PSS parts for passivating and improving the electrical properties of PEDOT:PSS films [13, 14]. OSCs fabricated with modified PEDOT:PSS are expected to be enhanced. PEDOT:PSS film preparation can be performed using several techniques such as dip-coating, spin-coating, and convective deposition [15, 16]. The dip-coating process requires large initial materials, while spin-coating causes a high loss of initial material by spinning out. On the other hand, the convective deposition can solve these problems. It requires low initial materials and causes low material loss; hence, its application to prepare PEDOT:PSS films.

2. Experiments

Starting materials, including poly(3,4-ethylenedioxythiophene)-poly(styrene sulfonate) (PEDOT:PSS, PH1000), poly[*N*-9′-heptadecanyl-2,7-carbazole-alt-5,5-(4′,7′-di-2-thienyl-2′,1′,3′-benzothiadiazole)] (PCDTBT), and phenyl C_{70} butyric acid methyl ester ($PC_{70}BM$), were purchased from Ossila, UK. ZnI_2 (≥98%) was purchased from Sigma-Aldrich, Singapore. All chemicals were used as received.

Fluorine doped-tin oxide (FTO, Sigma-Aldrich, Singapore, surface resistivity ~7 Ω/sq) substrates were cleaned with alconox detergent, de-ionized (DI) water, and isopropanol for 30 min each using an ultrasonic cleaner. Prior to deposition, the cleaned substrates underwent surface treatment with oxygen plasma (Ossila, Pathum Thani, Thailand). The ZnI_2 additive was dissolved into DI water for an initial concentration of 0.1 M, followed by stirring for 1 h, to obtain the final ZnI_2 solution. The ZnI_2 solution was then mixed into PEDOT:PSS for 0, 1, 2, and 4 vol%. The mixture was stirred for 30 min to form a homogeneous PEDOT:PSS aqueous solution. For PEDOT:PSS film deposition, 20 μl of the aqueous solution was deposited onto FTO substrates using a convective deposition technique, followed by heating at 120 °C for 30 min, to obtain PEDOT:PSS films. These films were then used as HTL for OSC application. The OSC structures of PEDOT:PSS/

PCDTBT:$PC_{70}BM$/TiO_x/Al were fabricated as described in prior work [15].

Current density-voltage (*J-V*) characteristics of OSCs were measured under the standard irradiation of 100 mW/cm^2 from a solar simulator (G2V pico, Pathum Thani, Thailand) to evaluate OSC performance. A cross-sectional image was acquired by a scanning electron microscope (SEM, JSM-6610 LV, JEOL, Bangkok, Thailand). The root-mean-square (RMS) surface roughness was examined by an atomic force microscope (AFM, Asylum Research MFP-3D, Bangkok, Thailand). The surface chemical element was investigated using X-ray photoelectron spectroscopy (XPS, Kratos, Axis ultra DLD, Bangkok, Thailand). Sheet resistance was measured using a four-point probe measurement (Ossila, Pathum Thani, Thailand). The contact angle was measured using a contact angle measurement system (a homemade setup with 500× microscope, Nakhon Pathom, Thailand). The optical transmittance was recorded by an ultraviolet-visible (UV-Vis) spectrophotometer (UV-3101 PC, Shimadzu, Nakhon Pathom, Thailand). The chemical structure was investigated using Fourier transform infrared (FTIR) spectroscopy (Spectrum Two, PerkinElmer, Nakhon Pathom, Thailand). Crystalline structures were characterized using X-ray diffractometry (XRD, D8 Advance, Bruker, Nakhon Pathom, Thailand) using a Cu K_α radiation wavelength (λ) of 1.5406 Å.

3. Results and discussion

The photovoltaic characteristics of OSCs fabricated with PEDOT:PSS films were analyzed by measuring current density – voltage (*J-V*) curves, as shown in Figure 1. The measurement was carried out using at least three repeated samples for each condition. The power conversion efficiency (*PCE*) was then calculated using the Equations (1) and (2) [15–17]:

$$PCE\,[\%] = \frac{J_{sc} \cdot V_{oc} \cdot FF}{P_{in}} \cdot 100 \tag{1}$$

$$FF = \frac{J_{max} \cdot V_{max}}{J_{sc} \cdot V_{oc}} \tag{2}$$

where J_{sc} is the short-circuit current density, V_{oc} is the open-circuit voltage, *FF* is the fill factor, P_{in} is the incident solar power from the solar simulator, J_{max} is current density at the maximum power point, and V_{max} is the voltage at the maximum power point. All photovoltaic parameters are summarized in Table 1.

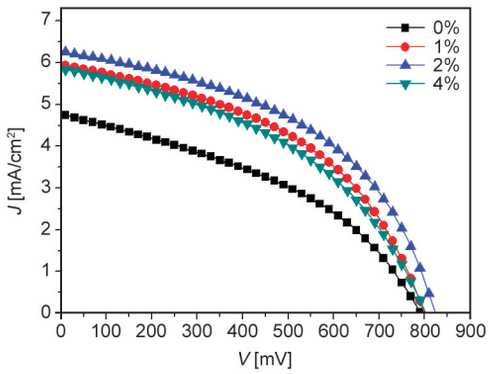

Figure 1. *J-V* curves of OSCs fabricated with PEDOT:PSS films at different ZnI_2 additive volumes.

It was found that OSC devices fabricated with ZnI_2-mixing PEDOT:PSS films demonstrate higher *PCE*s compared with the pristine PEDOT:PSS films. The *PCE*s slightly increase as ZnI_2 additive increases for 1–2 vol%, whereas 4 vol% ZnI_2 additive results in decreased *PCE* and J_{sc}. To investigate the correlation between photovoltaic parameters, plots of J_{sc}, V_{oc}, *FF*, and *PCE* as a function of ZnI_2 additive volume are shown in Figure 2. *PCE* trends are consistent with J_{sc}, V_{oc}, and *FF*, indicating that all photovoltaic parameters were improved for PEDOT:PSS mixed with ZnI_2 additive. This improvement is due to the reduced recombination in OSC devices [18], which is caused by the efficient hole transport efficiency. Note that the increase in V_{oc}, might also be attributed to the small change in the chemical structure of PEDOT:PSS in the presence of the ZnI_2 additive. In comparison with the other works mentioned above [9–12], the *PCE* of OSC in this work demonstrates low *PCE*s, which might be due to different fabrication methods [19]. However, the ZnI_2-mixing condition can enhance *PCE* for OSC application. For the 2 vol% ZnI_2-mixing conditions, it reveals the maximum *PCE* for OSC devices, implying the optimum condition. Therefore, it was further investigated as a representative of the modified PEDOT:PSS films in comparison with the pristine PEDOT:PSS films.

Table 1. Photovoltaic parameters of OSCs fabricated with PEDOT:PSS films at a different volumetric percentage of ZnI_2 additive mixtures.

ZnI_2 additive volume [%]	J_{sc} [mA/cm^2]	V_{oc} [mV]	*FF* [–]	*PCE* [%]
0	4.77±0.94	785±19	0.41±0.01	1.52±0.35
1	5.96±0.76	793±15	0.46±0.01	2.18±0.33
2	6.28±0.72	818±5	0.47±0.01	2.42±0.35
4	5.86±0.57	797±12	0.44±0.01	2.03±0.25

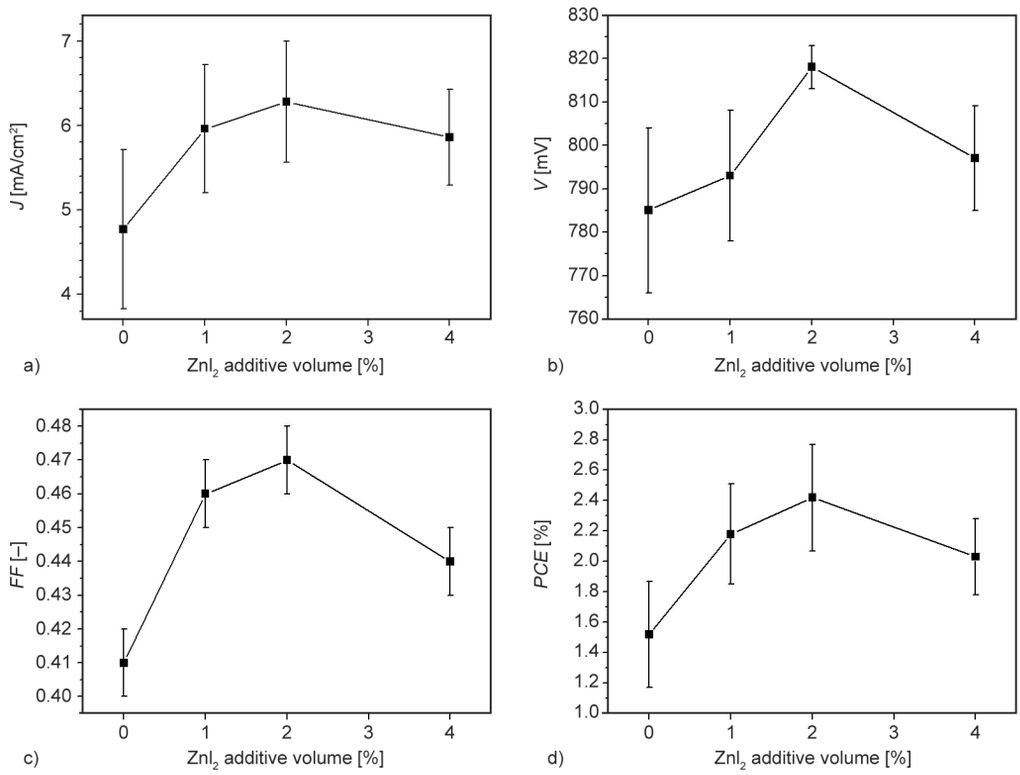

Figure 2. Photovoltaic parameters of OSCs fabricated with PEDOT:PSS films as function of ZnI_2 additive volume: a) J_{sc}, b) V_{oc}, c) *FF*, and d) *PCE*.

The cross-sectional SEM images in Figure 3 demonstrate that the interfaces between pristine PEDOT:PSS films and FTO substrates were not found. On the other hand, the junction between modified PEDOT:PSS and FTO layers was clearly observed. This indicates the different dynamic coating nature for pristine and modified PEDOT:PSS. To examine the surface roughness of PEDOT:PSS films, AFM was carried out. RMS roughness values of 8.80 and 15.03 nm were obtained for pristine and modified films, respectively. The roughness for modified films shows a higher value than that for the pristine films, indicating a higher surface area for modified films in comparison to the pristine films. The results imply that the interfacial contact has increased for OSC fabrication. This improvement leads to the high hole transport pathway and facilitates enhanced hole collection performance between PEDOT:PSS/PCDTBT:PC_{70}BM interfaces [20], which causes a higher current density for OSC devices.

The XPS measurement in Figure 4 shows the S(2p) peak of PEDOT:PSS films. The binding energy peak at around 167.8 eV corresponds to the sulfur atoms in PSS, whereas the peaks at around 163.5–164.7 eV represent the sulfur atoms in PEDOT [21, 22]. The intensity of S(2p) peaks for modified films is higher than that of pristine films, indicating that PEDOT:PSS chains reorient and change to compact layered PEDOT:PSS films. To examine the change of modified PEDOT:PSS films, PSS to PEDOT ratios were analyzed by calculating the peak areas for PSS and PEDOT peaks. The integrated S(2p) peak

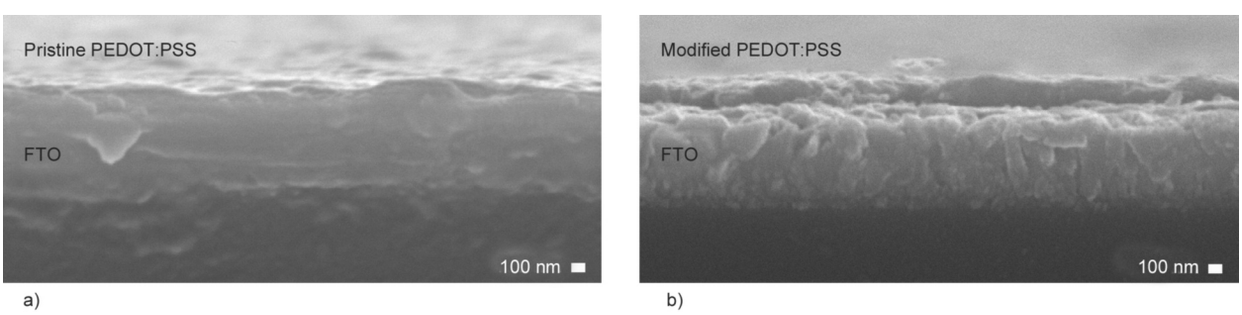

Figure 3. Cross-sectional images of a) FTO/pristine PEDOT:PSS and b) FTO/modified PEDOT:PSS.

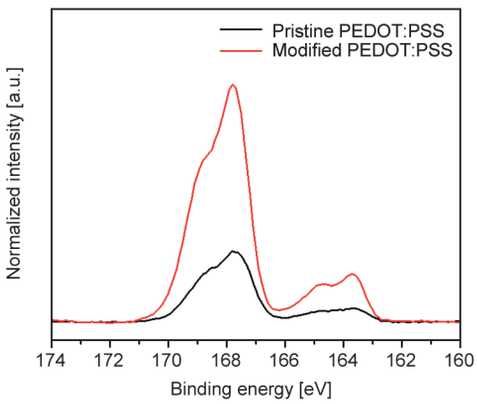

Figure 4. XPS spectra of pristine and modified PEDOT:PSS films.

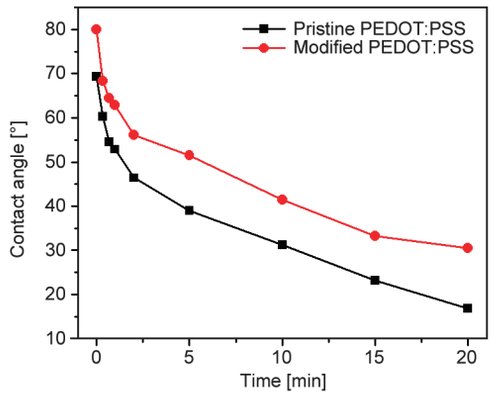

Figure 5. Contact angle measurement of pristine and modified PEDOT:PSS films.

areas were 4.69:1 and 4.15:1 for pristine and modified films, respectively. The decrease in integrated S(2p) peak areas for modified films points to the depletion of PSS from the surface of modified films by around 12% compared with pristine films [23]. This behavior implies re-orientation and re-interaction of PEDOT:PSS in the presence of the ZnI_2 additive. It can be interpreted that PEDOT:PSS films modified with ZnI_2 additive were changed as the compact formation and PSS depletion from the film's surfaces. This behavior can enhance hole transport efficiency in OSC devices, primarily due to the increase of hole-conducting PEDOT to insulating PSS ratios. The efficient hole transport behavior also suppresses the recombination effect, which results in an increased J_{sc} and V_{oc} for OSC devices [24].

To investigate the impact of PSS depletion on electrical property, sheet resistance was measured using a four-point probe measurement. The measurement presents the sheet resistance value of 81.16±1.96 and 69.59±3.78 Ω/sq for the pristine and modified films, respectively. The modified films exhibit a 14% decrease in sheet resistance in comparison with the pristine one, which nearly correlates to the decrease in PSS to PEDOT ratios. Moreover, the decrease in sheet resistance corresponds to the increase in J_{sc} value for OSC devices. Therefore, the improved electrical property of the modified films is considered an effective factor for enhancing the *PCE* of OSCs in this work. Moreover, PSS depletion also changes the surface wettability of PEDOT:PSS films as shown by the contact angle measurement results in Figure 5. The contact angle measured within a drop of DI water features hydrophilic properties for both pristine and modified films, and it slightly decreases for longer intervals. The contact angle of modified films, however, demonstrates a higher value compared to that of pristine films. This is due to the depletion of water-soluble PSS parts from the surface of modified PEDOT:PSS films, leaving higher ratios of non-soluble PEDOT parts at the film's surfaces and causing a higher contact angle.

The transmittance spectra in Figure 6 were measured to evaluate the optical impact on OSC performance. The transmittance spectra significantly decrease for the modified films in comparison with the pristine ones. This feature could be affected by the incorporation of ZnI_2, which is caused by the dense and compact structure of PEDOT:PSS in accordance with XPS results. Although low transmittance was obtained for the modified films, the *PCE* of the OSC device increased. This may be due to the fact that the active layer (PCDTBT:$PC_{70}BM$) can respond to the incident light, even with a low intensity [25]. Note that the low intensity of incident light also prevents the burn-in loss of V_{oc}, which maintains stability for OSC devices. This result suggests that the significant

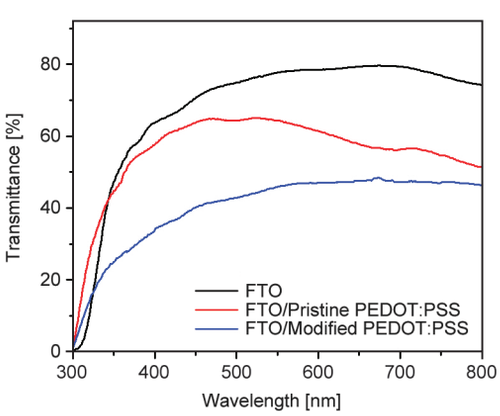

Figure 6. Optical transmittance of FTO, FTO/pristine PEDOT:PSS films, and FTO/modified PEDOT:PSS films.

factor for enhanced OSC devices is not transmittance but resistance.

To analyze the structures of the PEDOT:PSS films, FTIR spectra, and XRD patterns were performed. The observation of the PEDOT:PSS structures were determined from the FTIR peaks (Figure 7a) at 1010 and 665 cm^{-1} for the SO^{3-} symmetric stretching of PSS and the C–S stretching of PEDOT, respectively [26]. The results confirm the PEDOT:PSS structure for both pristine PEDOT:PSS and modified PEDOT:PSS films. In terms of the other peaks, the broad peaks at 3860–3670 and 1440 cm^{-1} were assigned to the O–H stretching and bending vibrations, respectively. The peak at 1725 cm^{-1} represents the C=O stretching vibration of the COOH group. The peaks at 1365 and 1220 cm^{-1} represent the C–O stretching vibration. Figure 7b shows the XRD patterns of pristine PEDOT:PSS and modified PEDOT:PSS films deposited on FTO substrates. The XRD peak of PEDOT:PSS at 2θ~17.10° was found for both pristine and modified PEDOT:PSS films contributed from PSS, indicating PEDOT:PSS crystalline structures [27]. The small XRD peak corresponds to PEDOT (2θ~25.80°), which was found for only pristine PEDOT:PSS films but disappeared for the modified PEDOT:PSS films. This is due to the interaction between the ZnI_2 additive and PEDOT:PSS molecules. Note that the ZnI_2 structures were not detected by XRD characterization [28]. This is possibly due to the insufficient ZnI_2 additive for PEDOT:PSS-ZnI_2 mixtures or to ZnI_2 being distributed into the PEDOT:PSS matrices.

4. Conclusions

PEDOT:PSS were modified with the ZnI_2 solution and coated onto an FTO substrate for application as a hole transporting layer in OSCs. The average power conversion efficiency was enhanced from 1.52 to 2.42%. This enhancement was found to be in correspondence with the rough surface of modified PEDOT:PSS, which improves the interfacial contact between PEDOT:PSS and PCDTBT:PC_{70}BM. This improvement leads to the high hole transport pathway and facilitates improved hole collection performance, which thus leads to a higher current density for OSC devices. Moreover, the ZnI_2 plays a role in the depletion of insulating PSS from the film's surface. This behavior causes lower sheet resistance and results in an increased J_{sc} and V_{oc} for OSC devices. Therefore, the improved interfacial contact and depletion of PSS are considered a synergistic function for OSC enhancement.

Acknowledgements

This work was supported by the Research Promotion and Technology Transfer Center (RPTTC), Faculty of Liberal Arts and Science, Kasetsart University Kamphaeng Saen Campus; and the Department of Physics, Faculty of Liberal Arts and Science, Kasetsart University Kamphaeng Saen Campus.

References

[1] Xu W., Ma X., Son J. H., Jeong S. Y., Niu L., Xu C., Zhang S., Zhou Z., Gao J., Woo H. Y., Zhang J., Wang J., Zhang F.: Smart ternary strategy in promoting the performance of polymer solar cells based on bulk-heterojunction or layer-by-layer structure. Small, **18**, 2104215 (2022). https://doi.org/10.1002/smll.202104215

[2] Xu C., Jin K., Xiao Z., Zhao Z., Yan Y., Zhu Z., Li X., Zhou Z., Jeong S. Y., Ding L., Woo H. Y., Yuan G., Zhang F.: Efficient semitransparent layer-by-layer organic photovoltaics via optimizing wide bandgap and narrow absorption polymer layer thickness. Solar RRL, **6**, 2200308 (2022). https://doi.org/10.1002/solr.202200308

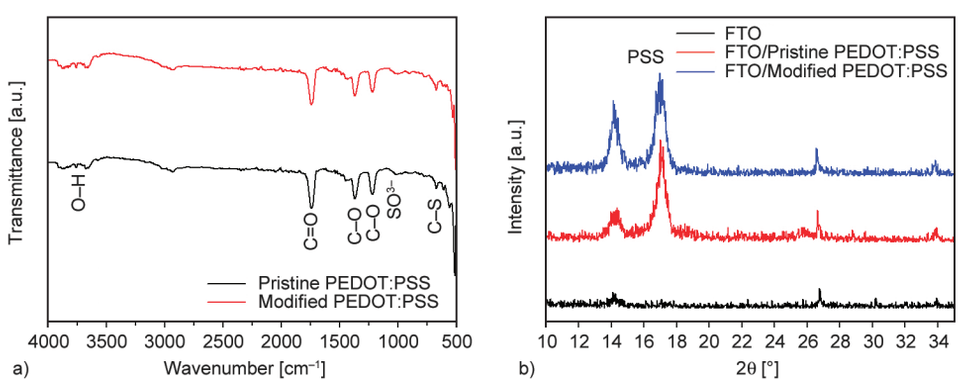

Figure 7. Structural analysis of pristine and modified PEDOT:PSS films: a) FTIR spectra and b) XRD patterns.

[3] Zhao X., Liu M., Yang K., Zhao Z., Wang J., Zhou Z., Ma X., Zhang F.: Photomultiplication type organic photodetectors with different response characteristics under forward or reverse bias. Organic Electronics, **108**, 106587 (2022).
https://doi.org/10.1016/j.orgel.2022.106587

[4] Wang X., Sun Q., Gao J., Wang J., Xu C., Ma X., Zhang F.: Recent progress of organic photovoltaics with efficiency over 17%. Energies, **14**, 4200 (2021).
https://doi.org/10.3390/en14144200

[5] Alamer F. A., Beyari R. F.: Overview of the influence of silver, gold, and titanium nanoparticles on the physical properties of PEDOT:PSS-coated cotton fabrics. Nanomaterials, **12**, 1609 (2022).
https://doi.org/10.3390/nano12091609

[6] Ong G. L., Ong T. S., Yap S. L., Liaw D-J., Tou T. Y., Yap S. S., Nee C. H.: A brief review of nanoparticles-doped PEDOT:PSS nanocomposite for OLED and OPV. Nanotechnology Reviews, **11**, 1870–1889 (2022).
https://doi.org/10.1515/ntrev-2022-0104

[7] Liu X., Shi X-L., Zhang L., Liu W-D., Yang Y., Chen Z-G.: One-step post-treatment boosts thermoelectric properties of PEDOT:PSS flexible thin films. Journal of Materials Science and Technology, **132**, 81–89 (2023).
https://doi.org/10.1016/j.jmst.2022.05.047

[8] Hu L., Song J., Yin X., Su Z., Li Z.: Research progress on polymer solar cells based on PEDOT:PSS electrodes. Polymers, **12**, 145 (2020).
https://doi.org/10.3390/polym12010145

[9] Hussain S., Liu H., Hussain M., Mehran M. T., Kim H-S., Jung J., Vikraman D., Kang J.: Development of MXene/WO_3 embedded PEDOT:PSS hole transport layers for highly efficient perovskite solar cells and X-ray detectors. International Journal of Energy Research, **46**, 12485–12497 (2022).
https://doi.org/10.1002/er.8020

[10] Gemeiner P., Pavličková M., Hatala M., Hvojnik M., Homola T., Mikula M.: The effect of secondary dopants on screen-printed PEDOT:PSS counter-electrodes for dye-sensitized solar cells. Journal of Applied Polymer Science, **139**, 51929 (2022).
https://doi.org/10.1002/app.51929

[11] Wan J., Fan X., Li Y., Li P., Zhang T., Hui K. N., Huang H., Kang K., Qian L.: High-efficiency flexible organic photovoltaics and thermoelectricities based on thionyl chloride treated PEDOT:PSS electrodes. Frontiers in Chemistry, **9**, 807538 (2022).
https://doi.org/10.3389/fchem.2021.807538

[12] Xu W., Zhu X., Ma X., Zhou H., Li X., Jeong S. Y., Woo H. Y., Zhou Z., Sun Q., Zhang F.: Achieving 15.81% and 15.29% efficiency of all-polymer solar cells based on layer-by-layer and bulk heterojunction structures. Journal of Materials Chemistry A, **10**, 13492–13499 (2022).
https://doi.org/10.1039/D2TA02914F

[13] Zhang S., Hu J., Huang S., Zhang J., Lyu M., Lu H., Zhu J.: ZnI_2 post-processing of $CsPbBr_3$ quantum dots for red, stable, and low-threshold amplified spontaneous emission. Applied Physics Letters, **120**, 221101 (2022).
https://doi.org/10.1063/5.0091905

[14] Tian C., Han X., Zhao Y., Sun Z., Hou C., Wang H., Qi J., Li Y., Jia W., Zhang Q.: Anion effect on properties of Zn-doped $CH_3NH_3PbI_3$ based perovskite solar cells. Solar Energy Materials and Solar Cells, **233**, 111400 (2021).
https://doi.org/10.1016/j.solmat.2021.111400

[15] Ritruksa M., Wongrerkdee S., Lohawet K., Kaewprajak A., Kumnorkaew P., Wongrerkdee S.: Surface modification of PEDOT: PSS film by chemical vapor texturing process for enhanced organic photovoltaics. Surfaces and Interfaces, **21**, 100716 (2020).
https://doi.org/10.1016/j.surfin.2020.100716

[16] Wongrerkdee S., Ritruksa M., Phattum S., Lohawet K., Kaewprajak A., Kumnorkaew P., Wongrerkdee S.: PEDOT:PSS film preparation and characterization using convective deposition system controlled by arduino microcontroller for organic photovoltaic application. Engineering Journal, **25**, 335–341 (2021).
https://doi.org/10.4186/ej.2021.25.2.335

[17] Wongrerkdee S., Moungsrijun S., Pimpang P., Hongsith K., Choopun S.: Linking bridge improvement of ZnO/N719 interfaces *via* ammonia treatment for efficiency enhancement of dye-sensitized solar cell. Surfaces and Interfaces, **23**, 100991 (2021).
https://doi.org/10.1016/j.surfin.2021.100991

[18] Niu Z., Zheng E., Dong H., Tosado G. A., Yu Q.: Manipulation of PEDOT:PSS with polar and nonpolar solvent post-treatment for efficient inverted perovskite solar cells. ACS Applied Energy Materials, **3**, 9656–9666 (2020).
https://doi.org/10.1021/acsaem.0c01194

[19] Neukom M., Züfle S., Jenatsch S., Ruhstaller B.: Optoelectronic characterization of third-generation solar cells. Science and Technology of Advanced Materials, **19**, 291–316 (2018).
https://doi.org/10.1080/14686996.2018.1442091

[20] Ge B., Zhou Z. R., Wu X. F., Zheng L. R., Dai S., Chen A. P., Hou Y., Yang H. G., Yang S.: Self-organized Co_3O_4-$SrCO_3$ percolative composites enabling nanosized hole transport pathways for perovskite solar cells. Advanced Functional Materials, **31**, 2106121 (2021).
https://doi.org/10.1002/adfm.202106121

[21] Reza K. M., Gurung A., Bahrami B., Mabrouk S., Elbohy H., Pathak R., Chen K., Chowdhury A. H., Rahman M. T., Letourneau S., Yang H-C., Saianand G., Elam J. W., Darling S. B., Qiao Q.: Tailored PEDOT:PSS hole transport layer for higher performance in perovskite solar cells: Enhancement of electrical and optical properties with improved morphology. Journal of Energy Chemistry, **44**, 41–50 (2020).
https://doi.org/10.1016/j.jechem.2019.09.014

[22] Zhao Z., Wu Q., Xia F., Chen X., Liu Y., Zhang W., Zhu J., Dai S., Yang S.: Improving the conductivity of PEDOT:PSS hole transport layer in polymer solar cells *via* copper(II) bromide salt doping. ACS Applied Materials and Interfaces, **7**, 1439−1448 (2015). https://doi.org/10.1021/am505387q

[23] Mengistie D. A., Wang P-C., Chu C-W.: Effect of molecular weight of additives on the conductivity of PEDOT:PSS and efficiency for ITO-free organic solar cells. Journal of Materials Chemistry A, **1**, 9907–9915 (2013). https://doi.org/10.1039/c3ta11726j

[24] Syed A. A., Poon C. Y., Li H. W., Zhu F.: A sodium citrate-modified-PEDOT:PSS hole transporting layer for performance enhancement in inverted planar perovskite solar cells. Journal of Materials Chemistry C, **7**, 5260–5266 (2019). https://doi.org/10.1039/C8TC06043F

[25] Züfle S., Hansson R., Katz E. A., Moons E.: Initial photo-degradation of PCDTBT:$PC_{70}BM$ solar cells studied under various illumination conditions: Role of the hole transport layer. Solar Energy, **183**, 234–239 (2019). https://doi.org/10.1016/j.solener.2019.03.020

[26] Paul G., Verma S., Jalil O., Thakur D., Pandey C. M., Kumar D.: PEDOT: PSS-grafted graphene oxide-titanium dioxide nanohybrid-based conducting paper for glucose detection. Polymers for Advanced Technologies, **32**, 1774–1782 (2021). https://doi.org/10.1002/pat.5213

[27] Rwei S-P., Lee Y-H., Shiu J. W., Sasikumar R., Shyr U. T.: Characterization of solvent-treated PEDOT:PSS thin films with enhanced conductivities. Polymers, **11**, 134 (2019). https://doi.org/10.3390/polym11010134

[28] Kariper I. A.: Optical and structural properties of zinc iodine thin films. Optical Materials, **44**, 78–83 (2015). https://doi.org/10.1016/j.optmat.2015.03.012